Effects of Interpatient Variance on Microwave Breast Images: Experimental Evaluation

Declan O'Loughlin, Bárbara L. Oliveira, Martin Glavin, Edward Jones and Martin O'Halloran

Abstract— Microwave breast imaging has seen significant developments in recent years, including new clinical trials and formation of a number of spin-out companies. Although many algorithms for microwave breast imaging have been developed, there are significant challenges in translating these algorithms to the clinic. For example, movement due to patient breathing can affect the scan, and both the breast and breast abnormalities vary significantly from patient to patient. As breast density is a known independent risk factor for cancer and cancerous tumours have different shapes and margins to benign tumours, the effect of interpatient variance on the microwave image is important. This work analyses the effect on image quality of tumour shape, size and breast density. Using the diverse and representative BRIGID experimental dataset, images of a variety of tumours are compared to images without tumours present. This work suggests that it is difficult to distinguish images with and without tumours present using existing metrics.

I. Introduction

In recent years, a number of clinical evaluations of microwave breast imaging have been published [1]–[6]. An on-going trial with the MARIA® system is being commercialised by Micrima Ltd. (Bristol, the UK) has shown equivalent sensitivites to mammography with over 200 cases [1], [7]. Particularly encouraging results have been demonstrated in dense breasts, a known independent risk factor for breast cancer [1], [8]. Another commercial imaging system is being developed by Microwave Vision Group (Villebon-sur-Yvette, France) with clinical trials commencing in the very near future [9] and comprehensive reviews of these clinical trials have been published [10], [11].

The increasing amount of commercial activity and clinical evidence available motivates researchers to consider the substantial challenges in translating microwave radar-based imaging to the clinic. For example, the breast varies substantially from patient to patient in size, shape and composition [12]. Additionally, tumours vary significantly in clinical practice, and shape and boundary in particular is an important factor influencing the clinical decision [13].

This work evaluates the effect of breast composition and tumour shape and size on microwave radar-based images. The diverse, experimental BRIGID breast phantom set is used, containing breast phantoms modelling a variety of densities that can be combined with different tumour phantoms modelling both benign and malignant cases. This allows the effect of breast composition for a given tumour phantom to be estimated as well as the effect of tumour size and shape to be analysed.

Additionally, this modular breast phantom set allows the images of the phantom with and without the tumour present to be compared, which is important when designing software to display the image to the clinician.

National University of Ireland Galway, Ireland.

II. Methods

The BRIGID phantom set used in this work has been described in [14]. Breast composition can vary substantially from patient to patient, for example, one study with 240 women aged between 35 and 82 found that the volume fraction of glandular tissues varies between 0% and 50% [12]. The most dense phantom in this work contains 30% glandular tissue, greater than 90% of patients in [12].

Tumour shape, in particular the tumour margin, is an important factor for assessing malignancy. Benign tumours are characterized by smooth, regular borders whereas malignant tumours are characterized by irregular or spiculated borders as they are growing [13]. The tumour phantoms in this work are modelled based on these principles and are shown in [14].

Backscattered data were acquired in the frequency domain using a ZNB40 2 port vector network analyser (VNA) and ZN-Z84 24 port switching matrix. As described in [15], 24 antennas were distributed around a 7 cm radius hemisphere, collecting 276 independent channels. The antennas operating characteristics are described fully in [16] and have been previously been demonstrated in a sixteen-antenna array with patients in [5].

Rotational subtraction was used to isolate the tumour response as has been used in recent clinical trials [1]. Multistatic Delay-and-Sum from the MERIT toolbox [17], with parameter search algorithms described in [18]–[20] were used for reconstruction. Imaging was completed in the frequency domain using 51 frequency points linearly spaced between 2 GHz and 4 GHz.

Considering operational microwave imaging systems that have been used with patients with disease [1], [2], [4], a number of different display methods have been used. The image is thresholded and normalised with respect to the image amplitude in [1], [4]. DICOM-compatible images are displayed to the clinician in [1]. Other studies have displayed the entire image and have suggested that it may be possible to use the image amplitude to determine if an abnormality is present or not [2].

TABLE I

Metrics for three tumours of increasing spiculation (low, intermediate and high) and no tumour in a breast phantoms of increasing glandular fraction (GF) up to thirty percent. The tumours are between 13 mm and 18 mm in diameter. Tumour images where the tumour is not found in the correct location are shown as —. In general, the SCR, SMR and maximum amplitude decrease as the heterogeneity increases, although there is no discernable trend in FWHM. FWHM is measured in millimetres; maximum amplitude, SCR and SMR in decibels.

GF	Spiculation	FWHM	Max.	SCR	SMR
0%	No tumour	8	-67.2	1.4	12.8
	Low	8.7	-28.4	6.5	23.0
	Inter.	8.7	-25.7	6.0	21.9
	High	8.7	-29.8	4.2	23.0
10%	No tumour	18.7	-63.4	2.3	11.0
	Low	8.0	-27.6	3.7	16.9
	Inter.	9.3	-24.5	2.1	14.9
	High	8.0	-25.2	2.9	11.6
20%	No tumour	10	-62.9	0.6	11.0
	Low	7.3	-41.3	3.4	16.5
	Inter.	7.3	-41.1	1.3	15.0
	High	8.0	-42.7	1.7	9.9
30%	No tumour	7.3	-58.7	2.0	15.0
	Low	—	—	—	—
	Inter.	10	-54.9	2.4	14.2
	High	—	—	—	—

The analysis in this work helps identify important image characteristics that can help distinguish tumour and no tumour cases.

III. Results

Four metrics were used to analyse the images of both tumour and no tumour cases:

- the signal-to-clutter ratio (SCR): the ratio of image maximum to the magnitude of the next response of most energy;
- the signal-to-mean ratio (SMR): the ratio of the image maximum to the image mean;
- the full-width at half-maximum (FWHM): an estimation of the extent of the response;
- and the maximum image amplitude.

Firstly, the effect of spiculation and breast density are considered in table I for tumour models L4, I12 and H18 from [14]. The images in fig. 1 correspond to the no tumour case (leftmost column) and the intermediate spiculated tumour (rightmost column). Each row corresponds to a phantom of increasing glandular fraction. A number of observations can be made considering, firstly, the tumour cases:

- performance decreases as the volume of glandular tissue increases, a finding consistent with previous experimental analysis [21]: the low and high spicu-

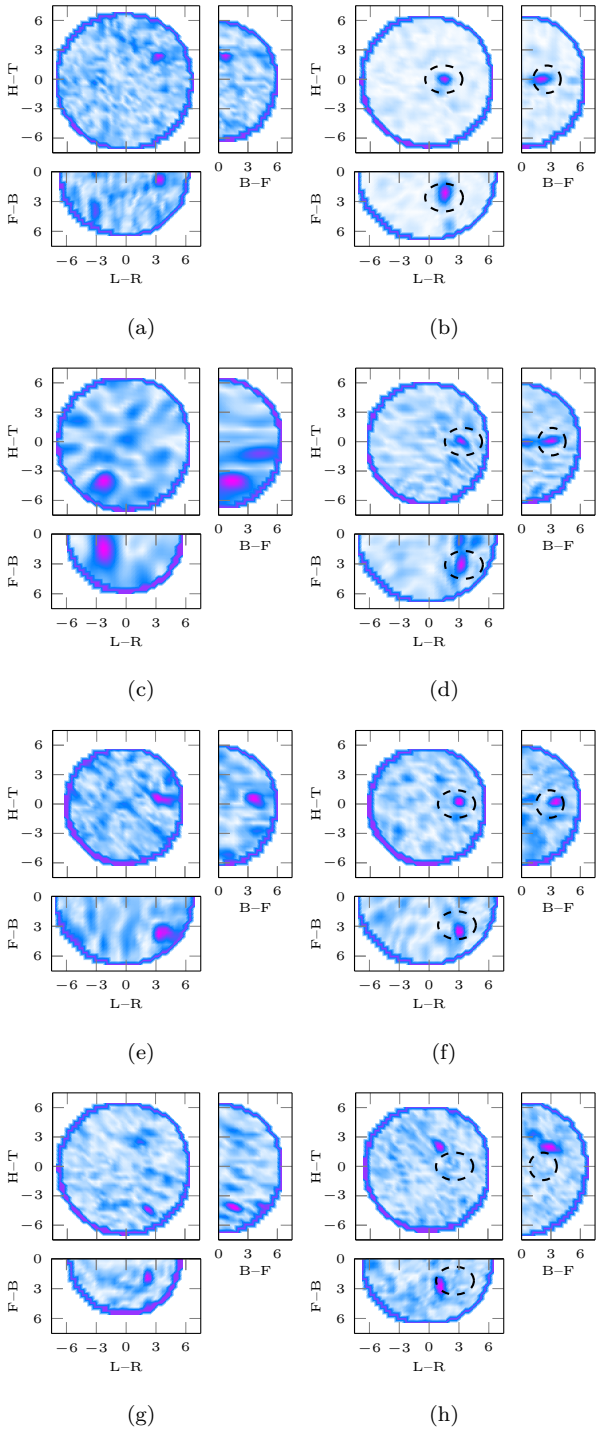

Fig. 1. Images with of four breast phantoms of increasing glandular fraction from 0% in row 1 to 30% in row 4. Axes are labelled as front (F), back (B), left (L), right (R), head (H) and toe (T) and all dimensions are in centimetres. Images without the tumour present are shown the leftmost column; images with the intermediate spiculated tumour from table I are shown in the rightmost column. Although the overall amplitude is much lower, images of glandular structures can appear similar to images of tumours, particularly in dense breasts, for example, images (e) and (f).

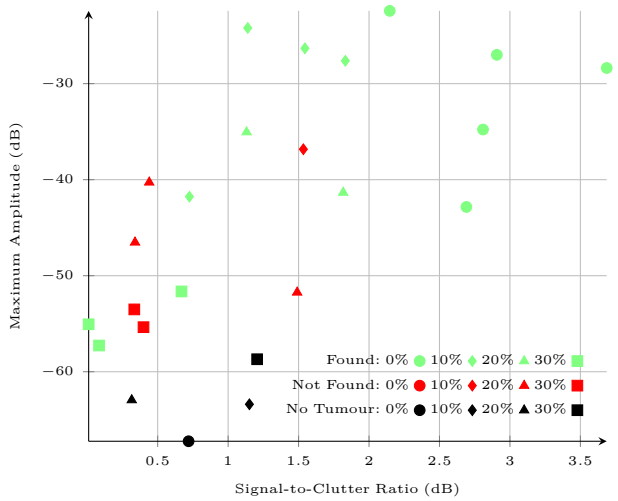

Fig. 2. Images of five spherical tumour phantoms of diameter between 5 mm and 20 mm in each of the four breast phantoms are compared. The fourteen detected tumour phantoms are shown in green, the six incorrectly located tumour phantoms are shown in red, and the images of the four breast phantoms without any tumours are shown in black. The maximum amplitude and SCR are more similar for tumour compared to no tumour images as the breast density increases.

lated tumours are not detected with 30% glandular tissue (table I);

- the FWHM does not change substantially with respect to either spiculation or glandular content;
- the SCR ratios are typically highest in the phantoms with least glandular tissue for the least spiculated tumour phantoms, and for 9 of the 10 detected tumours, the SCR is above the 1.5 dB threshold used in [1], [3];
- the SMR is also typically highest in the phantoms with the least glandular tissue;
- the maximum amplitude of tumour cases covers a wide range from −54.9 dB to −24.5 dB: image amplitude is highest with the least glandular content and, typically, for the least spiculated tumour phantom.

Comparing the tumour cases to the no tumour cases, it can be observed that:

- the maximum amplitude of the no tumour cases increases with density and can be similar to the tumour cases in the densest phantoms (−58.7 dB compared to −54.9 dB in a phantom with 30% glandular tissue);
- the no tumour cases have similar SCR, SMR and FWHM values to tumour cases in all phantoms;
- however, it can also be observed in fig. 1 that the maximum intensity of the image in the no tumour cases is very close to the edge of the imaging domain in all no tumour cases.

Finally, the maximum amplitude and SCR of five tumour phantoms of increasing size in each of the four breast phantoms are compared in fig. 2. Similar trends can be observed compared to the previous analysis:

- the maximum image amplitude and SCR tends to decrease as the glandular fraction increases for tumour cases;
- for no tumour cases, the maximum image amplitude tends to increase with the glandular fraction, due to increased reflections from the breast interior. This is the opposite to tumour cases where the higher dielectric properties of the dense breasts mean that reflections are lower in magnitude;
- and performance decreases as the glandular fraction increases, one tumour is not found when the glandular fraction is below 10% whereas five are not found when the glandular fraction is above 10%.

These results show that it is difficult to separate tumour images from no tumour images on SCR alone, but that the maximum image amplitude may be useful as was found in [2]. However, in dense breasts, the magnitude of tumour images can be much closer to the magnitude of no tumour images than for lucent breasts.

IV. Conclusions

In this work, the effect of tumour size and shape on image quality is assessed using a realistic experimental system, including rotational artefact removal and average dielectric properties estimation. Additionally, the effect of breast density on image quality using a realistic distribution of breast phantoms is investigated.

These results are consistent with previous experimental work from a number of systems showing that increasing glandular fraction in the breast phantom has a large impact on image quality. However, although as yet to be fully explained, results with the MARIA® system do not show this deterioration in performance in dense breasts [1].

Characteristics of images reconstructed with and without tumour phantoms are compared to help identify important metrics to preserve when displaying the image to the clinician. The images shown demonstrate how images of dense breast phantoms without tumours can appear similar to those of phantoms with tumours due to the increased reflections in the phantom. The data suggest that maximum image amplitude may be useful in distinguishing tumour and no tumour cases, although this is most challenging in breast phantoms with a high glandular fraction.

Future work is needed to examine these trends using patient images, where increased noise in the acquired data from patient movement may affect the maximum image amplitude even when no breast abnormalities are present. This work suggests that an optimal image display method needs to be identified that maximises the clinical efficacy in terms of sensitivity and specificity.

Acknowledgement

This work was supported by the Irish Research Council (GOIPG/2014/987), Science Foundation Ireland

(12/IP/1523) and the European Research Council (grant agreement number 637780).

References

[1] A. W. Preece, I. J. Craddock, M. Shere, et al., "MARIA M4: Clinical evaluation of a prototype ultrawideband radar scanner for breast cancer detection," Journal of Medical Imaging, vol. 3, no. 3, p. 033 502, Jul. 2016.

[2] E. C. Fear, J. Bourqui, C. F. Curtis, et al., "Microwave Breast Imaging With a Monostatic Radar-Based System: A Study of Application to Patients," IEEE Transactions on Microwave Theory and Techniques, vol. 61, no. 5, pp. 2119–2128, May 2013.

[3] F. Yang, L. Sun, Z. Hu, et al., "A large-scale clinical trial of radar-based microwave breast imaging for Asian women: Phase I," in Proceedings of the International Symposium on Antennas and Propagation (APSURSI), San Diego, CA, USA: IEEE, Jul. 9–14, 2017, pp. 781–783.

[4] H. Song, S. Sasada, T. Kadoya, et al., "Detectability of Breast Tumor by a Hand-held Impulse-Radar Detector: Performance Evaluation and Pilot Clinical Study," Scientific Reports, vol. 7, no. 1, p. 16 353, Dec. 2017.

[5] E. Porter, M. Coates, and M. Popović, "An Early Clinical Study of Time-Domain Microwave Radar for Breast Health Monitoring," IEEE Transactions on Biomedical Engineering, vol. 63, no. 3, pp. 530–539, Mar. 2016.

[6] Y. Kuwahara, "Microwave Imaging for Early Breast Cancer Detection," in New Perspectives in Breast Imaging, A. M. Malik, Ed., InTech, Oct. 2017.

[7] H. Massey, N. Ridley, I. Lyburn, et al., "Radiowave detection of breast cancer in the symptomatic clinic—a multi-centre study," in Proceedings of the International Cambridge Conference on Breast Imaging, Cambridge, UK, Jul. 3–4, 2017.

[8] N. Ridley, M. Shere, I. Lyburn, et al., "Cancer detection in dense tissue using radiofrequency imaging—a clinical evaluation," in Proceedings of the European Congress of Radiology Annual Meeting, Vienna, Austria: European Society of Radiology, Mar. 1–5, 2017.

[9] A. Fasoula, S. Anwar, Y. Toutain, et al., "Microwave vision: From RF safety to medical imaging," in Proceedings of the 11th European Conference on Antennas and Propagation (EuCAP), Paris, France: IEEE, Mar. 19–24, 2017, pp. 2746–2750.

[10] A. Modiri, S. Goudreau, A. Rahimi, et al., "Review of Breast Screening: Towards Clinical Realization of Microwave Imaging," Medical Physics, vol. 44, no. 12, e446–e458, Nov. 2017.

[11] D. O'Loughlin, M. O'Halloran, B. M. Moloney, et al., "Microwave Breast Imaging: Clinical Advances and Remaining Challenges," Transactions on Biomedical Engineering, no. 99, Feb. 2018.

[12] S.-Y. Huang, J. M. Boone, K. Yang, et al., "The characterization of breast anatomical metrics using dedicated breast CT," Med. Phys., vol. 38, no. 4, pp. 2180–2191, Apr. 1, 2011.

[13] B. L. Oliveira, M. O'Halloran, R. C. Conceição, et al., "Development of Clinically-Informed 3D Tumor Models for Microwave Imaging Applications," IEEE Antennas and Wireless Propagation Letters, vol. 15, pp. 1–1, 2015.

[14] B. L. Oliveira, D. O'Loughlin, M. O'Halloran, et al., "Microwave Breast Imaging: Experimental tumour phantoms for the evaluation of new breast cancer diagnosis systems," Biomedical Physics & Engineering Express, vol. 4, no. 2, Feb. 2018, 025036.

[15] D. O'Loughlin, B. L. Oliveira, M. A. Elahi, et al., "Parameter Search Algorithms for Microwave Radar-Based Breast Imaging: Focal Quality Metrics as Fitness Functions," Sensors, vol. 17, no. 12, Dec. 2017, Art. 2823.

[16] H. Bahramiabarghouei, E. Porter, A. Santorelli, et al., "Flexible 16 Antenna Array for Microwave Breast Cancer Detection," IEEE Transactions on Biomedical Engineering, vol. 62, no. 10, pp. 2516–2525, Oct. 2015.

[17] D. O'Loughlin, M. A. Elahi, E. Porter, et al., "Open-source software for microwave radar-based image reconstruction," in Proceedings of the 12th European Conference on Antennas and Propagation (EuCAP), London, the UK: IEEE, Apr. 9–13, 2018.

[18] D. O'Loughlin, M. Glavin, E. Jones, et al., "Optimisation of Confocal Microwave Breast Images using Image Focal Metrics," in Proceedings of the 22nd Bioengineering in Ireland (BINI), Galway, Ireland: Royal Academy of Medicine in Ireland, Jan. 22–23, 2016, pp. 39–39.

[19] D. O'Loughlin, F. Krewer, M. Glavin, et al., "Estimating average dielectric properties for microwave breast imaging using focal quality metrics," in Proceedings of the 10th European Conference on Antennas and Propagation (EuCAP), Davos, Switzerland: IEEE, Apr. 10–15, 2016, pp. 1–5.

[20] ——, "Focal quality metrics for the objective evaluation of confocal microwave images," International Journal of Microwave and Wireless Technologies, vol. 9, no. 07, pp. 1365–1372, Sep. 2017.

[21] M. Klemm, J. A. Leendertz, D. Gibbins, et al., "Microwave Radar-Based Breast Cancer Detection: Imaging in Inhomogeneous Breast Phantoms," IEEE Antennas and Wireless Propagation Letters, vol. 8, pp. 1349–1352, 2009.